Structure of the harmonic oscillator in the space of n-particle Glauber correlators

E. Zubizarreta Casalengua, J. C. López Carreño, E. del Valle, and F. P. Laussy

Citation: Journal of Mathematical Physics **58**, 062109 (2017); doi: 10.1063/1.4987023
View online: http://dx.doi.org/10.1063/1.4987023
View Table of Contents: http://aip.scitation.org/toc/jmp/58/6
Published by the American Institute of Physics

JOURNAL OF MATHEMATICAL PHYSICS **58**, 062109 (2017)

Structure of the harmonic oscillator in the space of *n*-particle Glauber correlators

E. Zubizarreta Casalengua,[1] J. C. López Carreño,[1] E. del Valle,[1] and F. P. Laussy[2,3,a)]

[1]*Departamento de Física Teórica de la Materia Condensada, Universidad Autónoma de Madrid, Madrid E-28049, Spain*

[2]*Faculty of Science Engineering, University of Wolverhampton, Wulfruna St., Wolverhampton WV1 1LY, United Kingdom*

[3]*Russian Quantum Center, Novaya 100, 143025 Skolkovo, Moscow Region, Russia*

(Received 5 December 2016; accepted 6 June 2017; published online 27 June 2017)

We map the Hilbert space of the quantum harmonic oscillator to the space of Glauber's *n*th-order intensity correlators, in effect showing "the correlations between the correlators" for a random sampling of the quantum states. In particular, we show how the popular $g^{(2)}$ function is correlated to the mean population and how a recurrent criterion to identify single-particle states or emitters, namely, $g^{(2)} < 1/2$, actually identifies states with at most two particles on average. Our charting of the Hilbert space allows us to capture its structure in a simpler and physically more intuitive way that can be used to classify quantum sources by surveying which territory they can access. *Published by AIP Publishing.* [http://dx.doi.org/10.1063/1.4987023]

INTRODUCTION

The formalization of quantum mechanics in the early days of its construction[1] led to the introduction of the Hilbert space as the structure to accommodate and unify the rules of Heisenberg to compute observables[2] and the wavefunction of Schrödinger to describe the quantum states.[3] To Einstein's reported observation that it would be enough to understand the electron, Dirac replied that "it would be enough if students could understand the harmonic oscillator."[4] This object indeed ranks as the foundation for much of our description of the world, not so much as the (quantum) mechanical object itself, but as the single mode of a bosonic field. In this way, light can be described as a collection of coupled harmonic oscillators, and such a basic notion as "coherence" was revolutionized in this workframe, changing from "a monochromatic field" (a single oscillator is excited) to "uncorrelated photons" (regardless of their origin).[5] In a modern understanding, a single mode of well defined frequency can be chaotic and a broadband, even a time-varying field, can be coherent. It is only because of the observed correlation in the physical observables between thermal and/or chaotic fields with broad linewidths that the identification of the two concepts came to be, which is still enduring to this day. With technology and the rising of photonics, however, the family of quantum states of the light field has been enlarged considerably with more examples to distinguish these two concepts than to associate them. In quantum optical terms, coherence is nowadays described by the Glauber correlators (we shall consider henceforth only a single bosonic mode a),

$$g^{(n)} \equiv \langle a^{\dagger n} a^n \rangle / \langle a^\dagger a \rangle^n \,, \tag{1}$$

where a is the annihilation operator (or "ladder operator") that removes one quantum from the Fock state $|n\rangle$ according to $a|n\rangle = \sqrt{n}|n-1\rangle$. The Glauber correlators are normalized quantities obtained from the ratio of observables,

$$G^{(n)} \equiv \langle a^{\dagger n} a^n \rangle \,. \tag{2}$$

a)Electronic mail: F.Laussy@wlv.ac.uk

As we will use the normalized form in our discussion, instead of $g^{(1)}$ which is unity, we will use as a first-order variable the normalization itself, that is, the mean population of the oscillator (average number of quanta),

$$n_0 \equiv G^{(1)} = \langle a^\dagger a \rangle . \tag{3}$$

These observables provide an essentially comprehensive description of the quantum state of a harmonic oscillator, through its n-particle fluctuation properties. In this text, we only consider the states and not their dynamics according to some Hamiltonian and/or Liouvillian equation of motion, so that all the correlators are same-time correlators. In a dynamical context, $g^{(1)}(\tau) \equiv \langle a^\dagger(0)a(\tau)\rangle/n_0$ becomes an important observable by itself (its decay time from unity is related to spectral coherence, that is, its departure from a single line). The $g^{(n)}$ correlators describe collective fluctuations at several orders, for instance, $g^{(2)}$ (the most widely used one) is related to the variance of the population according to $g^{(2)} = 1 + (\mathrm{Var}(n_0) - n_0)/n_0^2$. For Poisson fluctuations of the population, $\mathrm{Var}(n_0) = n_0$ and $g^{(2)} = 1$. The underlying quantum state is the coherent state[6] theorized by Sudarshan[7] and Glauber.[8] Sub-Poissonian fluctuations are characteristic of genuine quantum states of the field, i.e., with no classical analogues, epitomized by the Fock state.[9] Chaotic light, on the contrary, exhibits large fluctuations, with $g^{(2)} = 2$. The underlying quantum state is the thermal density matrix.[8] These correlators are also popularly known as the "nth-order quantum coherence functions."

CHARTING THE HILBERT SPACE

All our discussion so far has been well-known introductory material to quantum mechanics courses. In the following, we will study quantum states of the harmonic oscillator (that can be thought of as the single mode of a cavity) that go beyond the well-known particular cases through which we usually perceive the Hilbert space. The canonical basis for the space is provided by the Fock states $|n\rangle$. While we will ultimately be concerned with the complete space $\mathcal{H}_\infty$ of the Harmonic oscillator, it will be convenient to approach it through subspaces of at most N quanta,

$$\mathcal{H}_N = \left\{ \sum_{k=0}^{N} \alpha_k |k\rangle \; ; \; \left(\alpha_k \in \mathbb{C}\right) \wedge \left(\sum_{k=0}^{N} |\alpha_k|^2 = 1 \right) \right\} . \tag{4}$$

It is well known, since Pegg and Barnett's attempts to define a phase operator,[10] that working in a truncated Hilbert space of arbitrarily high maximum particle-number N allows us to get access to physical properties that become pathological in the infinite-dimensional space. We likewise consider truncated spaces that can later be enlarged in a limiting process, in which case $\mathcal{H}_\infty \equiv \bigcup_{N=0}^{\infty} \mathcal{H}_N$.

While Eq. (4) provides a comprehensive depiction of $\mathcal{H}_N$, it is a deceiving picture that keeps hidden much of the structure of the space. This is this structure which we shall attempt to clarify in the following through its visualization in terms of $g^{(n)}$ observables. The need for such an analysis is motivated by the recent interest in exciting optical targets with the new sources of quantum light[11,12] made available by the progress in quantum sources engineering.[13] When driving a harmonic oscillator with quantum light, one can bring the system to a state that falls outside the known particular cases, even though a considerable zoology has already been established. Indeed, beyond the most famous cases already presented (thermal and coherent), the literature describes a large family of quantum states for the harmonic oscillators, with Gaussian states,[14] predominantly squeezed states,[15] but also more exotic families, such as cat states, i.e., superposition of coherent states[16] in various possible combinations,[17] two-photon coherent states,[18] Fock-added coherent states,[19] excited two-photon coherent states[20] and their generalization,[21] binomial[22] and negative binomial states,[23] etc. The quantum world being such a bizarre place, even such a simple operation as subtracting a state to itself has inspired profuse discussions.[24] In most cases, the classifications follow from a particular scheme that allows one to engineer the corresponding states. As such, they do not provide a picture of the Hilbert space that is both simple and comprehensive and that would be practical to survey which regions of the Hilbert space have already been covered, are the easiest to access, which are its boundaries, if any, and what areas remain to be explored. This is such a picture that we provide based on the particles' joint-correlation properties.

A first simplification following from our approach that relies on observables—Eqs. (1)–(3)—that are sensitive to diagonal elements $P_k \equiv |\alpha_k|^2$ only, is to lift the distinction between *pure states*, i.e., those of the form of Eq. (4) that can be written with a wavefunction, and *mixed states*, i.e., statistical superpositions of these that are consequently of the following type:

$$\rho = \sum_{k=0}^{N} P_k |k\rangle\langle k| + \sum_{\substack{k,l=0 \\ k\neq l}}^{N} P_{k,l} |k\rangle\langle l| \,, \tag{5}$$

with $P_{k,l} \in \mathbb{C}$ in general but $P_k \in \mathbb{R}$ (note that we write P_k instead of $P_{k,k}$). The mixed case is a generalization which reduces to the pure one when $P_{k,l} = \alpha_k \alpha_l^*$, and the second sum in Eq. (5) is redundant. A maximally mixed state on the other hand cancels altogether the second sum. The arbitrary case interpolates between these two situations corresponding to the degree of purity or coherence (depending on terminology). We will leave it to context or to cases of greater generality to decide which case is meant or useful. For instance, $\alpha_n = \exp(-|\alpha|^2/2)\alpha^n/\sqrt{n!}$ can be understood as both the coherent state and the random-phase coherent state[25] (with all off-diagonal elements as zero). We will likewise use the notation $\alpha_n = \sqrt{(1-\theta)\theta^n}$ (for $0 \leq \theta \leq 1$) for both the thermal state, which has null off-diagonal elements, and the pure state version that is actually also of interest, as the eigenstate of the Susskind-Glogower phase operator $(aa^\dagger)^{-1/2}a$,[26] in which case it is known as the "coherent phase state"[27] for its analogies with the coherent state, eigenstate of a; cf. Ref. 28 for a nice review. In any case, the important information for our exploration of the Hilbert space through particle fluctuations resides in the first sum of Eq. (5).

In $\mathcal{H}_N$ where the total number of excitations is truncated, $P_{N+m} = 0$ for $m \geq 1$ in Eq. (5); therefore, computing correlators (2) on states (5) yields the following sequence:

$$1 = \sum_{n=0}^{N} P_n \,, \tag{6a}$$

$$n_0 = \sum_{n=0}^{N} n P_n \,, \tag{6b}$$

$$G^{(2)} = \sum_{n=0}^{N} n(n-1) P_n \,, \tag{6c}$$

$$\vdots$$

$$G^{(N)} = \sum_{n=0}^{N} n(n-1)\cdots(n-N+1) P_n \,. \tag{6d}$$

In this case, there is a bijection $\mathcal{M}$ between the allowed $G^{(n)}$ correlators and the states uniquely defined through the first sum in Eq. (5). This can be written in a matrix form

$$\vec{G} = \mathbb{M}\vec{P} \tag{7}$$

between the vectors of $(N+1)$ elements $\vec{P} = (P_0, \ldots, P_N)^T$ and $\vec{G} = (1, n_0, G^{(2)}, \ldots, G^{(N)})^T$ with

$$\mathbb{M} = \begin{pmatrix} 1\ 1\ 1\ \ldots & 1 & 1 \\ 0\ 1\ 2\ \ldots & N-1 & N \\ 0\ 0\ 2\ \ldots & (N-2)(N-1) & N(N-1) \\ \ldots & \ldots & \ldots \\ 0\ 0\ 0\ \ldots & 0 & N(N-1)\cdots 1 \end{pmatrix}, \tag{8}$$

which, being upper-triangular, allows us to solve Eq. (7) by backward Gaussian substitution

$$P_{N-k} = \frac{1}{(N-k)_{N-k}} \left\{ G^{(N-k)} - \sum_{k'=N-k+1}^{N} (N-k)_{k'} P_{k'} \right\}, \tag{9}$$

where $(n)_k = \prod_{p=0}^{k-1}(n-p) = \langle n|a^{\dagger k}a^k|n\rangle$. This result can be expressed in an explicit recursive form by developing all the coefficients,

$$P_i = \sum_{j\geq i}^{N} (-1)^{i+j} \frac{G^{(j)}}{i!(j-i)!}, \tag{10}$$

for $0 \leq i \leq N$. This is the inverse relation of Eq. (6).

The expression holds true for any N and in a limiting process gets extended to the case $N \to \infty$. This relation can also be obtained through the method of generating functions.[29] Now that this relationship between P_k probabilities and $G^{(n)}$ correlators is settled, we are ready to approach the Hilbert space through the $g^{(n)}$ observables. Namely, we consider how a distribution of states from $\mathcal{H}_N$ is mapped in the space charted by $g^{(n)}$. We will call the latter space $\mathcal{G}_N$. Given that $0 \leq P_n \leq 1$ for all n, and their sum being unity by normalization, one can foresee constraints for the correlators, only at the level of "correlations between the correlators," e.g., are they all large or small together or is it on the opposite possible to have arbitrarily high values of $g^{(3)}$ for vanishing $g^{(2)}$? And if so, are such states in "equal numbers" than those of the opposite trend? We answer these questions by providing the density of states in the correlator space $\mathcal{G}_N$. Namely, we want to know how a distribution of points in $\mathcal{H}_N$ is mapped into $\mathcal{G}_N$.

Since the Fock state basis Eq. (4) is intuitive, it is natural to consider a uniform distribution in $\mathcal{H}_N$ as a fair representation of all the quantum states. For instance, the Hilbert space $\mathcal{H}_2$ is a 2D triangle in the 3D space (P_0, P_1, P_2) (see Fig. 1) and all the quantum states of at most two particles can be conveniently represented by the uniform distribution over this geometry, namely, a constant distribution of value $2/\sqrt{3}$ (the inverse area of an equilateral triangle of side $\sqrt{2}$). If a point is sampled randomly from this space, corresponding to choosing one of the quantum states of the form $\alpha_0|0\rangle + \alpha_1|1\rangle + \alpha_2|2\rangle$ with the same probability as any other, we then ask what is the probability that this state will have a given population and second-order correlation (all higher orders are zero since such states have at most two particles). From Eqs. (6), it is easy to see that the population lies between 0 and 2 and also that $0 \leq G^{(2)} \leq 2$, both maximised when $P_2 = 1$ and all other $P_n = 0$. It is not difficult, though less immediate, to show that $g^{(2)}$ is positive but unbounded (the possibility for two particles to exhibit arbitrarily large superbunching is also known from the dynamics of bosonic cascades[30]). Mathematically, this means that n_0 and $G^{(2)}$ can vary independently between 0 and 2. To know if there is some degree of correlation between them, we consider the distribution of states in the $(n_0, g^{(2)})$ space.

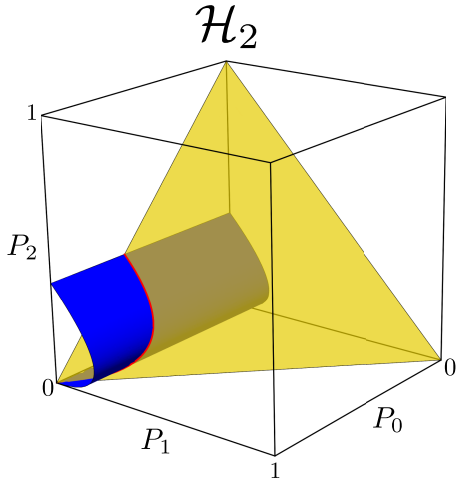

FIG. 1. The two-particle Hilbert space $\mathcal{H}_2$ in the canonical Fock basis P_k of probabilities for the state $|k\rangle$ is mapped on an equilateral triangle (yellow). A uniform sampling in this triangular space is a good representation of all the possible quantum states with at most two particles. The blue surface shows the states of constant $g^{(2)}$ (namely, $g^{(2)} = 1.3$) so that its intersection with the yellow triangle, shown as the red line, captures all the normalized physical quantum states with the corresponding $g^{(2)}$. The "measure" (here length) of this line correspond to their density in the space.

The quantum states with a given n_0 are found as the intersection between the triangle of normalized states in (P_0, P_1, P_2) with the plane of equation $P_1 + 2P_2 - n_0 = 0$. Similarly, the states with a given $g^{(2)}$ are the intersection of the same supporting triangle with the ellipsoid $(P_1 + 2P_2)^2 - 2P_2/g^{(2)} = 0$, shown as the blue surface in Fig. 1. The constant $g^{(2)}$ states in $\mathcal{H}_2$ are consequently those identified by the red line in Fig. 1. This turns the question of the density of states in $\mathcal{G}_N$ into a problem of measuring surfaces in hyperspaces: the measure, i.e., total area or volume related to a certain manifold, has the same value regardless of which parametrization (or metric) is chosen. This is tackled in differential geometry with the first fundamental form $\mathbb{F}$ that provides the trajectory in one space that is parametrically defined in the other. The regions that are thus connected are, in general, hypersurfaces. The relation reads

$$\mathbb{F}_{k,k'} = \partial_{G^{(k)}}\vec{P} \cdot \partial_{G^{(k')}}\vec{P}, \tag{11}$$

where $1 \leq k, k' \leq N$ and $\cdot$ is the scalar product between the $\partial\vec{P}$ vectors. As the transformation Eq. (7) is linear, the elements of $\mathbb{F}$ are constant, namely, they are given by $\mathbb{F}_{k,k'} = \sum_{i\leq k,k'} (-1)^{k+k'} / [i!^2 (k - i)!(k' - i)!]$. An element of (hyper)surface in $\mathcal{H}_N$ is related to the corresponding element in $\mathcal{G}_N$ by $\mathcal{P}_G dn_0 \cdots dG^{(N)} = (\sqrt{|\mathbb{F}|}/A_N) dP_0 \cdots dP_N$ with $\mathcal{P}_G$ as the density of probability, A_N as the volume of the Hilbert space $\mathcal{H}_N$ that, being a simplex of dimension $N + 1$, reads

$$A_N = \frac{\sqrt{N+1}}{N!}, \tag{12}$$

and the value of $|\mathbb{F}|$ can be computed from Eq. (11) and is found in terms of the superfactorial $\mathrm{sf}(N) = \prod_{i=0}^{N} i!$ as

$$\sqrt{|\mathbb{F}|} = \frac{\sqrt{N+1}}{\mathrm{sf}(N)}. \tag{13}$$

While the computation is conveniently performed with $\vec{G}$, we are eventually interested in the space of normalized correlators $g^{(n)}$, that we will call $\mathcal{g}_N$. A summary of the spaces involved and the notations to identify them is given in Table I. There is another bijection $\mathcal{N}$ from $\mathcal{G}_N$ to $\mathcal{g}_N$ that simply involves powers of n_0 as $(n_0, G^{(2)}, \ldots, G^{(N)}) = (n_0, n_0^2 g^{(2)}, \ldots, n_0^N g^{(N)})$. The Jacobian for this transformation from $\mathcal{G}_N$ to $\mathcal{g}_N$ reads

$$J = \left|\frac{\partial G^{(i)}}{\partial g^{(j)}}\right| = \begin{vmatrix} 1 & 0 & 0 & 0 \ldots & 0 \\ 2n_0 g^{(2)} & n_0^2 & 0 & 0 \ldots & 0 \\ 3n_0^2 g^{(3)} & 0 & n_0^3 & 0 \ldots & 0 \\ \ldots & \ldots & \ldots & \ldots & \ldots \\ N n_0^{N-1} g^{(N)} & 0 & 0 & 0 \ldots & n_0^N \end{vmatrix}$$
$$= \prod_{p=2}^{N} n_0^p = n_0^{(N^2+N-2)/2}. \tag{14}$$

TABLE I. Summary of notations for the various spaces introduced, and their corresponding joint densities of probability $\mathcal{P}$. $\mathcal{H}_N$ is the Hilbert space truncated to $N \in \mathbb{N}$ particles in the Fock basis. $\mathcal{G}_N$ is the corresponding space in the basis of unnormalized correlators $G^{(N)}$ and $\mathcal{g}_N$ in the space of Glauber correlators $g^{(n)}$. The densities of probability are such that for a uniform sampling, A_N is the volume of the Hilbert space $\mathcal{H}_N$, $\mathbb{F}$ is the first fundamental form, and J is the Jacobian of the transformation between the correlators and their normalized form. Their expressions are given in Eqs. (12) and (13). Θ is nonzero only if there is a physical state that provides the joint variables of the $\mathcal{P}$ functions.

Subspace	Probability
$\mathcal{H}_N$	$\mathcal{P}(P_0, P_1, \ldots, P_N) = (1/A_N)\Theta(\mathcal{H}_N)$
$\mathcal{G}_N$	$\mathcal{P}_G(n_0, G^{(2)}, \ldots, G^{(N)}) = (\sqrt{\lvert\mathbb{F}\rvert}/A_N)\Theta(\mathcal{G}_N)$
$\mathcal{g}_N$	$\mathcal{P}_g(n_0, g^{(2)}, \ldots, g^{(N)}) = (J\sqrt{\lvert\mathbb{F}\rvert}/A_N)\Theta(\mathcal{g}_N)$

This finally brings us to one of the main quantities of this text: the joint density of probability $\mathcal{P}_g\left(n_0, g^{(2)}, \ldots, g^{(N)}\right)$. Specifically, the probability that a state randomly picked from $\mathcal{H}_N$ has corresponding correlators $n_0, \ldots, g^{(N)}$ in an infinitesimal hypervolume $dn_0 \cdots dg^{(N)}$ is $\mathcal{P}_g dn_0 \cdots dg^{(N)}$. Bringing all the results above together, this density of probability is found as

$$\mathcal{P}_g\left(n_0, g^{(2)}, \ldots, g^{(N)}\right) = \frac{n_0^{(N^2+N-2)/2}}{\mathrm{sf}(N-1)}\Theta(\mathcal{g}_N)\,, \tag{15}$$

where $\Theta(\mathcal{g}_N) \equiv \mathbf{1}_{\mathcal{N}\circ\mathcal{M}(\mathcal{H}_N)}$ is the support for the image of $\mathcal{H}_N$ through the bijection $\mathcal{N}\circ\mathcal{M}$, i.e., it is 1 if there exists a state with joint-correlators n_0, $g^{(2)}$, …, $g^{(n)}$ and is 0 otherwise. The subset $\mathcal{N}\circ\mathcal{M}(\mathcal{H}_N)$ remains to be made explicit and its identification represents the core of the problem. It is already notable, however, that for physical states, $\mathcal{P}_g$ is independent of all the correlators except the population n_0.

We now turn to particular cases to apply and illustrate these results. In each case, the following procedure holds: a uniform distribution of states in the space $\mathcal{H}_N$ leads to a corresponding distribution in $\mathcal{g}_N$ given by Eq. (15). The space $\mathcal{g}_N$ itself is bounded when projected onto its n_0 axis. The boundaries are found from re-arranging the inequalities $0 \le P_i \le 1$ with P_i given by Eq. (10) to read as inequalities for the correlators instead. Marginal distributions can be obtained that provide the distribution of quantum states in subspaces of interest [e.g., $(n_0, g^{(n)})$].

THE TWO-PARTICLE HILBERT SPACE $\mathcal{H}_2$

We consider first the simplest space distinct from that of the two-level system ($\mathcal{H}_1$ is the Hilbert space of a qubit and its complete characterization is textbook material[31]). Namely, $\mathcal{H}_2$, the space spanned by $|0\rangle$ (vacuum), $|1\rangle$, and $|2\rangle$, has dimension 3 and can be fully represented geometrically in a 3D Euclidean space. We have already used this space to illustrate the nature of the Hilbert space in the P_k and $G^{(k)}$ bases in Fig. 1.

Equation (10) reads in this case

$$P_0 = 1 - n_0 + \frac{n_0^2 g^{(2)}}{2}\,, \tag{16a}$$

$$P_1 = n_0(1 - n_0 g^{(2)})\,, \tag{16b}$$

$$P_2 = \frac{n_0^2 g^{(2)}}{2}\,, \tag{16c}$$

with $0 \le P_k \le 1$. The reverse relations are familiar from the definitions of the following observables:

$$P_0 + P_1 + P_2 = 1\,, \tag{17a}$$

$$P_1 + 2P_2 = n_0\,, \tag{17b}$$

$$\frac{2P_2}{(P_1 + 2P_2)^2} = g^{(2)}\,. \tag{17c}$$

The corresponding joint density of probability $\mathcal{P}_g$, i.e., yielding the probability of finding a state with given $(n_0, g^{(2)})$ from a uniform sampling in the Hilbert space, is

$$\mathcal{P}_g(n_0, g^{(2)}) = n_0^2\,\Theta\left(\mathcal{g}_2\right)\,, \tag{18}$$

where $\Theta\left(\mathcal{g}_2\right)$ vanishes if $\left(n_0, g^{(2)}\right) \notin \mathcal{g}_2$. As already stated, there is no explicit dependency of $\mathcal{P}_g$ on $g^{(2)}$ once in $\mathcal{N}\circ\mathcal{M}(\mathcal{H}_2)$. Since $\Theta(\mathcal{g}_2)$ is not 1 everywhere, there is, however, an implicit dependency through $\mathcal{g}_2$'s geometry. This space is found from Eqs. (16) and can be easily visualized as it is two-dimensional. The inequalities on P_k result in upper and lower boundaries for n_0 and $g^{(2)}$,

$$g^{(2)} \le \frac{1}{n_0}\,, \tag{19a}$$

$$g^{(2)} \ge \frac{\lfloor n_0 \rfloor(2n_0 - \lfloor n_0 \rfloor - 1)}{n_0^2}\,. \tag{19b}$$

The lower boundary for $g^{(2)}$, Eq. (19b), was already known[12] and applies to all $\mathcal{H}_N$. There is also, however, an upper boundary, Eq. (19a), that is specific to $\mathcal{H}_2$. Together, this constrains the states in $\mathcal{H}_2$ to be confined in the area shown in Fig. 2. The color code there is that given by Eq. (18) and shows that states uniformly distributed in $\mathcal{H}_2$ yield the largest density of probability in the edge $(n_0, g^{(2)}) = (2, 1/2)$, that is, the point corresponding to $|2\rangle$, since there is only one state with this mean population and states with similar populations also have a similar $g^{(2)}$. In contrast, there are many states with mean population 1, but their range of $g^{(2)}$ is limited (between 0 and 1), the probability to find one of them is thus intermediate. Finally, while there is also only one state with mean population zero (vacuum), states with similar populations can have any positive $g^{(2)}$, hence there is a small probability to find any such state. When disregarding the population, one finds that the antibunching with highest probability is that of the Fock state $|2\rangle$, i.e., $g^{(2)} = 1/2$, although another state will likely have been drawn in its place. If it would be uncorrelated, it would most likely have mean population 1.

The boundaries in $\mathcal{H}_2$ can also be written as

$$n_0 \leq \frac{1 - \sqrt{1 - 2g^{(2)}}\theta(1 - 2g^{(2)})}{g^{(2)}}, \tag{20}$$

where $\theta(x)$ is the Heaviside function. Regarding the upper bound, for a given allowed population, $0 \leq n_0 \leq 2$, $g^{(2)}$ cannot be larger than $1/n_0$. The lesser the population, the greater the maximum $g^{(2)}$ can be. This is consistent with results on superbunching obtained from bosonic cascades[30] that show that large bunching, $g^{(2)} \gg 2$, develop as the system gets close to vacuum. Even though the joint probability takes a simple form, the geometry of the Hilbert space when charted by the correlators

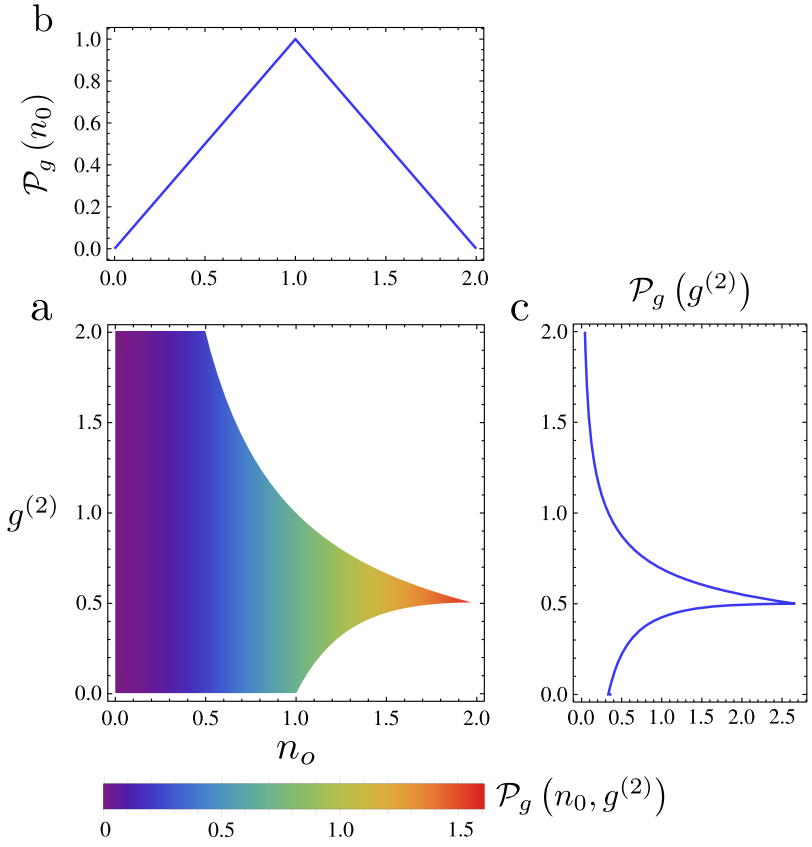

FIG. 2. Charting of the Hilbert space $\mathcal{H}_2$ (up to two-particles). (a) Probability distribution $\mathcal{P}_g(n_0, g^{(2)})$ of finding a quantum state with the corresponding population and $g^{(2)}$ from a random sampling in $\mathcal{H}_2$ (uniform distribution on the triangle in Fig. 1). The space exhibits both a lower and an upper boundary. (b) Distribution $\mathcal{P}_g(n_0)$ after averaging over $g^{(2)}$ and (c) distribution $\mathcal{P}_g(g^{(2)})$ after averaging over n_0. The space is unbounded in $g^{(2)}$, so that arbitrarily high superbunching can be realized, which requires vanishing populations.

has thus a complex form. This echoes in the reduced probability distributions that have a simple support, but complicated functional expressions. Both distributions, $\mathcal{P}_g(n_0)$ and $\mathcal{P}_g(g^{(2)})$, are obtained by integrating over the other observable. The first one provides the population distribution

$$\mathcal{P}_g(n_0) = \begin{cases} n_0, & \text{if } 0 \le n_0 \le 1, \\ 2 - n_0, & \text{if } 1 < n_0 \le 2 \end{cases} \tag{21}$$

and the other one provides the $g^{(2)}$ distribution

$$\mathcal{P}_g(g^{(2)}) = \begin{cases} \sqrt{\frac{8}{9}} \frac{(1 - \sqrt{1 - 2g^{(2)}} - g^{(2)})^{\frac{3}{2}}}{(g^{(2)})^3}, & \text{if } 0 \le g^{(2)} \le \frac{1}{2}, \\ \frac{1}{3(g^{(2)})^3}, & \text{if } g^{(2)} > \frac{1}{2}. \end{cases} \tag{22}$$

Both distributions are piecewise functions and are shown in Figs. 2(b) and 2(c). A random sampling in $\mathcal{H}_2$ is thus most likely to produce a state with one excitation if limiting to this observable and an antibunching of 1/2 if limiting to this observable. Jointly, however, the most likely $g^{(2)}$ remains 1/2 but now for a population of 2. This does not mean, however, that $|2\rangle$ is most probable, only that states close-by resemble it while states close-by, say, vacuum, are very different.

The states that lie on the boundaries of the Hilbert space (we will call them *coin states*) are a superposition of two of the three basis's Fock states,

$$\sqrt{1 - \frac{n_0}{2}}|\mu\rangle + \sqrt{\frac{n_0}{2}} e^{i\theta}|\nu\rangle \tag{23}$$

with $0 \le \mu, \nu \le 2$ such that $\mu \ne \nu$. The $|0\rangle$–$|1\rangle$ superpositions lie on the x-axis, $|0\rangle$–$|2\rangle$ define the upper boundary and $|1\rangle$–$|2\rangle$ define the lower boundary past $n_0 = 1$. The $n_0 = 0$ boundary is (set-topologically) open, that is, the states can get asymptotically close to, but without touching, the boundary. Other boundaries are closed since states (23) are part of $\mathcal{H}_2$. Note also that while $\mathcal{H}_2$ is bounded, g_2 is not, even though they are one-to-one connected.

THE THREE-PARTICLE HILBERT SPACE $\mathcal{H}_3$

The principle for $\mathcal{H}_3$ is the same as that for $\mathcal{H}_2$ but in a 4D space, since the space is enlarged with a new observable: the three-particle fluctuations $g^{(3)}$. This makes its visualization trickier. The results and their geometric interpretation are still valid, but instead of 2D surfaces one is now dealing with hypersurfaces.

Equation (10) reads in this case

$$P_0 = 1 - n_0 + \frac{n_0^2 g^{(2)}}{2} - \frac{n_0^3 g^{(3)}}{6}, \tag{24a}$$

$$P_1 = n_0 - n_0^2 g^{(2)} + \frac{n_0^3 g^{(3)}}{2}, \tag{24b}$$

$$P_2 = \frac{n_0^2 g^{(2)}}{2} - \frac{n_0^3 g^{(3)}}{2}, \tag{24c}$$

$$P_3 = \frac{n_0^3 g^{(3)}}{6}. \tag{24d}$$

One can check that if $g^{(3)} = 0$ ($P_3 = 0$), then the structure of $\mathcal{H}_2$ is recovered, as indeed $\mathcal{H}_2$ is a subspace of $\mathcal{H}_3$. The distribution of states is found as

$$\mathcal{P}_g(n_0, g^{(2)}, g^{(3)}) = \frac{n_0^5}{2} \Theta\left(g_3\right), \tag{25}$$

and as before, there is an explicit dependence only on the population, with an implicit dependence on $g^{(2)}$ and $g^{(3)}$ from the fact that the states are constrained to g_3. The boundaries for (n_0, $g^{(2)}$, $g^{(3)}$)

are complex. One can express them through the constrains on one variable set by the two others. This yields, for $g^{(2)}$ as a function of n_0 and $g^{(3)}$,

$$g^{(2)} \leq \frac{n_0 g^{(3)}}{2} + \frac{1}{n_0}\,, \tag{26a}$$

$$g^{(2)} \geq \max\left(n_0 g^{(3)}, \frac{n_0 g^{(3)}}{3} + \frac{2}{n_0} - \frac{2}{n_0^2}\right), \tag{26b}$$

and, for $g^{(3)}$ as a function of n_0 and $g^{(2)}$,

$$g^{(3)} \leq \min\left(\frac{g^{(2)}}{n_0}, \frac{3g^{(2)}}{n_0} - \frac{6}{n_0^2} + \frac{6}{n_0^3}\right), \tag{27a}$$

$$g^{(3)} \geq \max\left(0, \frac{2g^{(2)}}{n_0} - \frac{2}{n_0^2}\right), \tag{27b}$$

with $0 \leq n_0 \leq 3$ in both cases and $0 \leq g^{(2)}, g^{(3)}$ in general. Observe from Eq. (26a) how the bounding from $1/n_0$ allows $g^{(2)}$ to grow arbitrarily for vanishing populations. The equations apply for combinations of $(n_0, g^{(3)})$ and $(n_0, g^{(2)})$ that are possible in the first place, in which case the boundary for the third variable is as indicated and consist of sharp inequalities, meaning that the equality holds for some cases. If the combinations are not possible, the equations as well may become impossible, requiring, e.g., $g^{(3)} < 0$. The conditions for valid combinations define the projected spaces $(n_0, g^{(N)})$ and will be given later [cf. Eqs. (33)] as they apply for all N. Note that in $\mathcal{H}_2$, there is no such issue as the projected space is also the full space.

The boundary set by $g^{(2)}$ and $g^{(3)}$ on n_0 is the most complicated one, although it is only bounding from above. It is given in terms of two auxiliary functions, $f_1(g^{(2)}, g^{(3)})$ and $f_2(g^{(3)})$, defined in Appendix A [cf. Eqs. (A1)–(A3)] and reads

$$0 \leq n_0 \leq U(g^{(2)}, g^{(3)}) \tag{28}$$

with

$$U(g^{(2)}, g^{(3)}) \equiv \begin{cases} f_1(g^{(2)}, g^{(3)}), & \text{if } g^{(3)} \leq \frac{2}{9} \text{ and } g^{(2)} < f_2\left(g^{(3)}\right), \\ \dfrac{g^{(2)} - \sqrt{(g^{(2)})^2 - 2g^{(3)}}}{g^{(3)}}, & \text{if } g^{(3)} \leq \frac{2}{9} \text{ and } g^{(2)} \geq f_2\left(g^{(3)}\right), \\ \min[f_1, \dfrac{g^{(2)}}{g^{(3)}}], & \text{if } g^{(3)} \geq \frac{2}{9} \text{ and } g^{(2)} < \sqrt{2g^{(3)}}, \\ \dfrac{g^{(2)} - \sqrt{(g^{(2)})^2 - 2g^{(3)}}}{g^{(3)}}, & \text{if } g^{(3)} \geq \frac{2}{9} \text{ and } g^{(2)} \geq \sqrt{2g^{(3)}}. \end{cases} \tag{29}$$

The value 2/9 comes from $g^{(3)}$ of the Fock state $|3\rangle$.

These results are already difficult to visualize although still very near the ground state of the oscillator. They are shown in Fig. 3 in the full $\mathcal{H}_3$ space, where a single-sheet boundary encloses from above the space of allowed states up to three particles. In most practical situations, one is interested in pairwise correlations, so we address $\mathcal{H}_3$ more systematically through its projections into its subspaces. This is obtained for any combination of two variables by integrating over the third one. The expressions are bulky and would bring little enlightenment, so we keep them separate in the Appendix. In this way, we can find $\mathcal{P}_g(n_0, g^{(2)})$ [Eq. (A4)] and, for the new subspace now accessible, $\mathcal{P}_g(n_0, g^{(3)})$ [Eq. (A5)]. The exact solutions have the form of piecewise polynomial functions of their variables (cf. Appendix A). It is interesting to compare $\mathcal{P}_g(n_0, g^{(2)})$ for $\mathcal{H}_3$ to that calculated for $\mathcal{H}_2$, where it was providing the complete picture, while it is now averaged over $g^{(3)}$. The boundaries are also realized by Coin states of the form of Eq. (23), this time with $0 \leq \mu, \nu \leq 3$ (still with $\mu \neq \nu$). This is true as well for the new projected spaces $(n_0, g^{(3)})$.

As seen in Fig. 3, the Hilbert space is bounded for the population but is not bounded when not involving this parameter. This is due to intensity correlations of all orders being largely independent

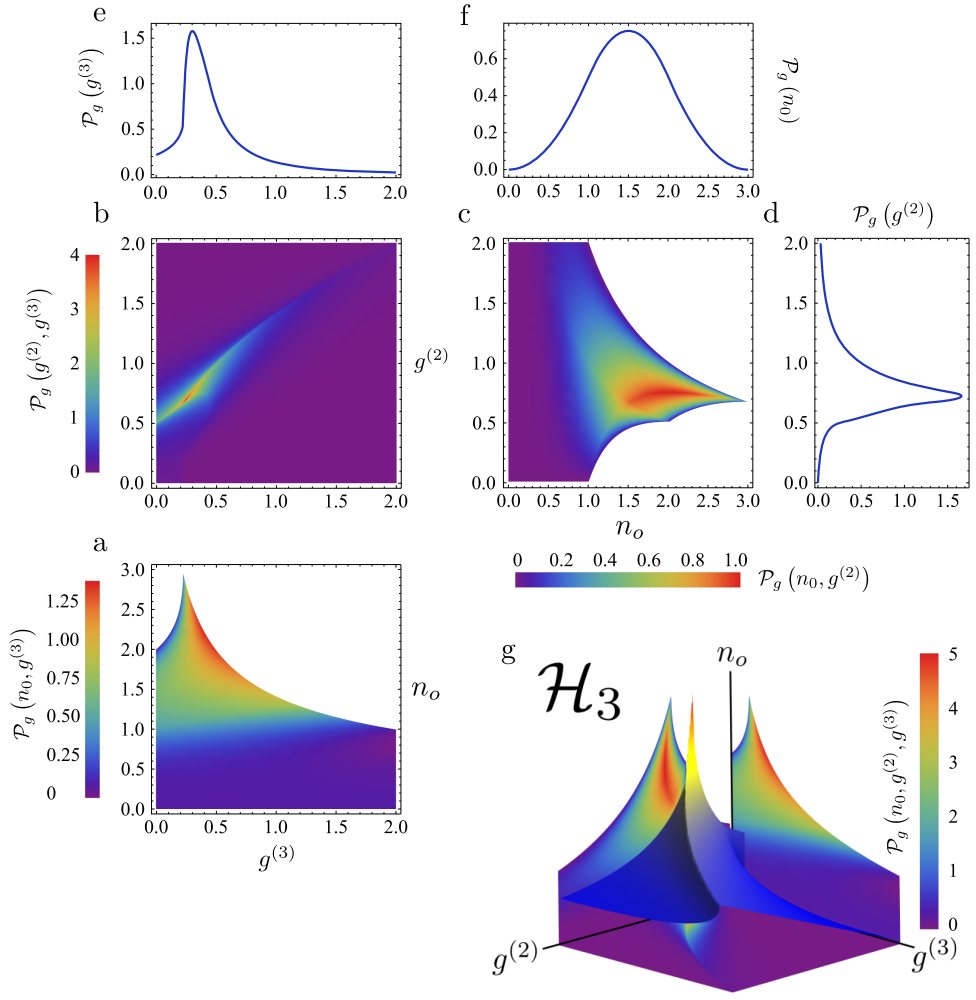

FIG. 3. Charting of the Hilbert space $\mathcal{H}_3$ (up to three-particles). (a) Density of probability distribution $\mathcal{P}_g(n_0, g^{(3)})$ after averaging over $g^{(2)}$ of finding a quantum state with the corresponding population and $g^{(3)}$ from a random sampling in $\mathcal{H}_3$ [uniform distribution in an hypervolume (not shown)]. The space exhibits both a lower and an upper boundary similar to $\mathcal{H}_2$. (b) Distribution $\mathcal{P}_g(g^{(2)}, g^{(3)})$ after averaging over n_0. This subspace is unbounded unlike those that involve the population. (c) Distribution $\mathcal{P}_g(n_0, g^{(2)})$ [cf. Fig. 2] after averaging over $g^{(3)}$. (d) Distribution $\mathcal{P}_g(g^{(2)})$, (e) $\mathcal{P}_g(g^{(3)})$, and (f) $\mathcal{P}_g(n_0)$. The latter distribution is of the Irwin-Hall type. (g) The complete distribution for $\mathcal{H}_3$ lives in a 3D space, shown here through its upper boundary along with the three projections on 2D spaces.

from the population, thus allowing a normalizing factor to make the quantity vanish or diverge (in contrast, $G^{(n)}$ are, like n_0, all bounded). As a result, all pairs of (positive) values for $(g^{(2)}, g^{(3)})$ are possible. One can get antibunched states of two particles that exhibit super three-particle bunching, and reciprocally superbunching at the two-particle level but three-particle antibunching, as well as, more expectedly, joint two/three antibunching and superbunching, respectively. Making more precise statements require us to be more specific on how the correlators reach their limits although one can be quite general regarding vacuum. Table II shows the upper bound U for the population, cf. Eqs. (28) and (29), in all the possible combinations for the limiting cases of $g^{(2)}$ and $g^{(3)}$. If at least one correlator diverges, then the boundary tends to 0, meaning that the state is dominated by vacuum, $P_0 \to 1$. One can otherwise turn to the density of probability for this subspace that quantifies the relative occurrence of all possible combinations. It reads

$$\mathcal{P}_g(g^{(2)}, g^{(3)}) = \frac{1}{12}\left[U(g^{(2)}, g^{(3)})\right]^6 \tag{30}$$

and is shown in Fig. 3(b).

TABLE II. Limiting cases of the population upper bound $U(g^{(2)}, g^{(3)})$ for all the possible combination of vanishing and diverging $g^{(2)}$ and $g^{(3)}$. In the bottom right cell, case (i) applies to $(g^{(2)})^2 > 2g^{(3)}$ while case (ii) applies to $(g^{(2)})^2 < 2g^{(3)}$. All cases except $g^{(2)} \to 0$ and $g^{(3)} \to 0$ lead to vanishing populations n_0. Similar analyses could be undertaken for higher correlators.

$U(g^{(2)}, g^{(3)})$	$g^{(2)} \to 0$	$g^{(2)} \to \infty$
$g^{(3)} \to 0$,	$1 + \frac{g^{(2)}}{2} - \frac{g^{(3)}}{6}$	$\frac{1}{g^{(2)}} + \frac{2g^{(3)}}{(g^{(2)})^3}$
$g^{(3)} \to \infty$	$\frac{g^{(2)}}{g^{(3)}}$	*i)* $\frac{1}{g^{(2)}} + \frac{2g^{(3)}}{(g^{(2)})^3}$ *ii)* $\frac{g^{(2)}}{g^{(3)}}$

Integrating one step further, the probability distribution for n_0 in $\mathcal{H}_3$ can be obtained from either Eq. (A4) or (A5) by integrating over the extraneous variable, which yields

$$\mathcal{P}_g(n_0) = \begin{cases} \frac{n_0^2}{2}, & \text{if } 0 \le n_0 \le 1\,, \\ -\frac{1}{2}\left(2n_0^2 - 6n_0 + 3\right), & \text{if } 1 < n_0 \le 2\,, \\ \frac{1}{2}\left(n_0^2 - 6n_0 + 9\right), & \text{if } 2 < n_0 \le 3 \end{cases} \tag{31}$$

that is plotted in panel (f) of Fig. 3. In a similar way, one can obtain from Eq. (A4) the reduced probability distribution for $g^{(2)}$ in $\mathcal{H}_3$, that is, another bulky expression [cf. Eq. (A6)] expressed in the piecewise form with the distribution itself being, as in the other cases, not only continuous but also everywhere differentiable. We could not find an analytical expression for $\mathcal{P}_g(g^{(3)})$ that is displayed in panel (e).

All the density of probabilities for all subspaces are shown in Fig. 3. The density plots are also shown as projections on their respective planes in the full 3D space. As one can see, the structure of the Hilbert space is intricate.

THE *N*-PARTICLE HILBERT SPACE $\mathcal{H}_N$

Further analytical results are not convenient (we refer to the Appendix A as an illustration of how the exact solutions quickly become cumbersome, already in $\mathcal{H}_3$). From the three-particle Hilbert space to higher dimensional ones, there is also a qualitative step. The inequality system can be handled for $\mathcal{H}_3$, in which case, polynomials of degree 3 are involved and their roots admit a closed form as given by the Cardano–Tartaglia formula. For $N \ge 4$, this method is not applicable (even if there exists the Ferrari formula for fourth degree polynomials). Nevertheless, some general characteristics can be inferred without closed-form solutions.

In all cases, the distributions for the population $\mathcal{P}_g(n_0)$ follow Irwin-Hall distributions (i.e., the distribution for the sum of N independent random variables with a uniform distribution),

$$\mathcal{P}_g(n_0) = \frac{1}{2(N-1)!} \sum_{k=0}^{N} (-1)^k \binom{N}{k} (n_0 - k)^{n-1} \operatorname{sgn}(n_0 - k)\,. \tag{32}$$

As a result, for large N, the distribution of population is normally distributed. This result is actually trivial and follows directly from our uniform sampling of the native Hilbert space (in the canonical Fock basis).

One can also generalize to all N, and thus also to the complete harmonic oscillator Hilbert space, the boundaries of g_N. They are constraining only when involving n_0, in which case they are given by (the proof is given in Appendix B)

$$g^{(k)} \leq \frac{(N-1)!}{(N-k)!}\frac{1}{n_0^{k-1}}, \tag{33a}$$

$$g^{(k)} \geq \frac{\lfloor n_0 \rfloor!}{(\lfloor n_0 \rfloor - k)! n_0^k}\left(1 + \frac{k(n_0 - \lfloor n_0 \rfloor)}{\lfloor n_0 \rfloor + 1 - k}\right). \tag{33b}$$

These equations are the ones that need to be satisfied for $N = 3$ to provide physical upper boundaries to Eqs. (26) and (27). As these are all sharp inequalities, one can easily find in this way the maximum correlators for a given population.

Equations (33) show that by increasing N, the upper boundary for $g^{(k)}$ wins territory in $\mathcal{G}_N$, unlike the lower boundary. This has the effect of retaining only a lower boundary in $\mathcal{H}_\infty$ that is shown for $g^{(2)}$ in Fig. 4. The dashed lines show the boundaries of the successive $\mathcal{H}_N$ spaces. The lower boundary of Fig. 4 shows that there exist states such that $n_0 > 1$ and $g^{(2)} < 1/2$ (with superpositions $\sqrt{p}|1\rangle + \sqrt{(1-p)}e^{i\theta}|2\rangle$ for $0 < p < 1$ lying on the frontier). This is an important observation as it invalidates a popular criterion in the literature that uses $g^{(2)} < 1/2$ as a criterion for single-particle states or, more frequently, single-photon emission.[32–37] Our map of the Hilbert space shows that the criterion $g^{(2)} < 1/2$ is proper to identify states with less than two particles on average, not one at any moment, as is the usual requirement for secure quantum protocols. The actual criterion for the latter is $g^{(2)} = 0$ and in the absence of an exact mathematical zero, one should turn to other criteria for single photon sources.[38]

Note also that while any combination $\left(g^{(k)}, g^{(k+n)}\right)$ (for $1 \leq n \leq N-k$) is allowed, this imposes constrains on other correlators, starting with n_0 regardless of the truncation N. In fact, if $g^{(k)} = 0$ for a particular k, it is easy to check that every higher order correlator as well as every coefficient P_n with $n \geq k$ is also necessarily zero. This effectively truncates the space. In the truncated space, not all combinations of correlators are allowed even if they satisfy Eqs. (33). In $\mathcal{H}_\infty$, however, all combinations are allowed, with open boundaries of the subspaces $\left(g^{(k)}, g^{(k+n)}\right)$, when $g^{(k)}, g^{(k+n)} \to 0$ (that is, excluding 0). A special case is the limit $n_0 \to 0$ (that has already been mentioned previously): no state except vacuum, $|0\rangle$, has population $n_0 = 0$. This result agrees with the fact that the density of probability $\mathcal{P}_N$ vanishes for $n_0 = 0$. A counterpart of Table II could be worked out. As the details of how the population vanishes might not be of importance, we only emphasize the following features that echo the results discussed for $\mathcal{H}_3$: in $\mathcal{H}_N$, if one correlator at least diverges, then the state gets dominated by vacuum: $P_0 \to 1$. This can be seen from the fact that this correlator, say of order k, is bounded from above in the $(n_0, g^{(k)})$ space, meaning that if $g^{(k)} \to \infty$, then $n_0 \to 0$. If no correlator diverges, including the case of all correlators vanishing, then the state can have a finite mean population. This vanishing population for a diverging correlator is not, however, true in general in $\mathcal{H}_\infty$. There, one can get diverging correlators for arbitrarily large populations. Consider, for instance, the case $(1-p)|0\rangle + p|n\rangle$, which, for any M as large as required, can be chosen to have population $np = M$ and $g^{(2)} = n(n-1)p/(np)^2 = (n-1)/(np)$ which tends to $1/p$ for n large enough. Thus, $g^{(2)} = 1/p = n/M$ can be made as large as we want, by considering n large enough (this is not possible if the space is

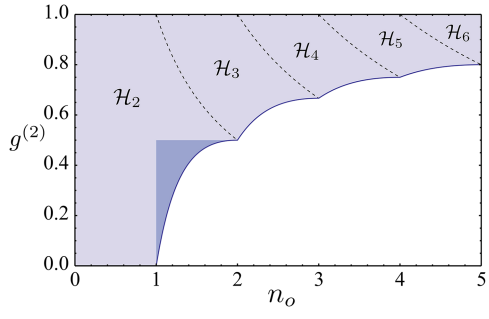

FIG. 4. Structure of the harmonic oscillator Hilbert space in the $(n_0, g^{(2)})$ subspace. There is a lower boundary but no upper boundary in $\mathcal{H}_\infty$. The dashed lines show the upper boundaries that do exist for bunching in the truncated spaces $\mathcal{H}_N$. The shaded region shows states with $g^{(2)} < 0.5$ and $n_0 > 1$.

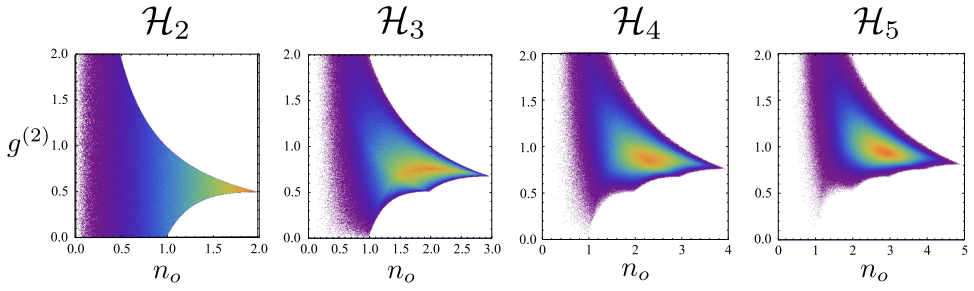

FIG. 5. Numerical distributions of states in the $(n_0, g^{(2)})$ subspace as obtained from Monte Carlo uniform sampling in $\mathcal{H}_N$ for $2 \leq N \leq 5$. The cases $N = 2$ and 3 match with the analytical solutions presented above. Larger N weaken quantum features such as the scars observed clearly in $\mathcal{H}_3$ that correspond to Coin states.

truncated). In turn, this makes p very small, showing that in this case again, the state is dominated by vacuum, but the excited state is now so largely populated that, on average, the population does not have to vanish. There are other ways to arrive to similar conclusions, showing in all that the structure of the Hilbert space is a subtle one and that one should resist temptations of constraining the quantum states from the behaviour of its Glauber correlators.

Finally, to gain an insight into higher-truncation spaces, we turn to numerical methods. This also provides a way to check the analytical results. In Fig. 5, we show the results of Monte Carlo sampling of states in the Hilbert spaces from $\mathcal{H}_2$ until $\mathcal{H}_5$ through their distribution in the $(n_0, g^{(2)})$ subspace. The numerical results reconstruct faithfully the distribution $\mathcal{P}_g(n_0, g^{(2)})$ for the case $N = 2$ and $N = 3$ for which we have provided analytical solutions. It is also interesting that with increasing N, one observes a blurring of the quantum features such as the scars made by the Coin states, clearly visible in $\mathcal{H}_3$, faintly so in $\mathcal{H}_4$ and essentially gone in $\mathcal{H}_5$, as well as the kinky features of the lower boundary. One witnesses in this way the typical fading of quantum correlations with a large number of particles.

CONCLUSIONS

We have mapped the states of the Hilbert space of the harmonic oscillator in the space of Glauber nth-order coherence function $g^{(n)}$ that captures the correlations of intensities at various orders in the number of particles. This allows us to chart the Hilbert space in a simple and visually appealing way, for instance, in the $(n_0, g^{(2)})$ subspace. We find that the Hilbert space has lower boundaries when featuring the population, such that for populations larger than one, some values of $g^{(n)}$ become impossible (no physical state can jointly provide them). There are no such restrictions when not involving the population, so that arbitrary superbunching at some order can occur concurrently with vanishing antibunching at some other order. For instance, one can find states with $g^{(2)} \to 0$, $g^{(3)} \gg 3!$, $g^{(4)} \to 0$, and $g^{(5)} \gg 5!$ (the values for superbunching are defined with respect to the thermal fluctuations) or indeed any combination, as long as the space has sufficiently high truncation. In the truncated space, where N is finite, not all combinations are possible as they need to belong to $\mathcal{g}_N$ which has complicated upper boundaries. Said otherwise, given a sequence of correlators that satisfy Eqs. (33), one can always produce corresponding states as long as higher order correlators $g^{(l)}$ for $l > N$ can also be chosen (typically, nonzero). If they are forced to be zero, they need to satisfy a more constrained condition involving a U function [cf. (29) for the case $N = 3$]. It must be pointed out in particular that the regions $g^{(2)} < 1/2$ and $n_0 > 1$ are populated, which invalidates a popular criterion for single-particle states or emission whenever $g^{(2)} < 1/2$. The suitable such criterion is the simpler (and harder to achieve) $g^{(2)} = 0$. What this criterion provides instead is a proof that the emission has at most two particles on average. In summary, our results provide a new, simple, and practical representation of the possible quantum states for the harmonic oscillator that should be of value, for instance, to classify quantum sources by considering which areas of the newly charted space they can reach.

ACKNOWLEDGMENTS

We acknowledge funding from the European Union through the ERC POLAFLOW and the Spanish MINECO under Contract No. FIS2015-64951-R (CLAQUE).

APPENDIX A: EXACT RESULTS

We list some of the exact and closed-form (but bulky) expressions for quantities discussed or plotted in the main text. They are obtained from the methods explained therein.

These are the auxiliary functions introduced to define the boundaries for the population in the Hilbert space $\mathcal{H}_3$ (f_0 is used in f_1),

$$f_0(g^{(2)},g^{(3)})=\sqrt{6(g^{(2)})^3(g^{(3)})^2-3(g^{(2)})^2(g^{(3)})^2-18g^{(2)}(g^{(3)})^3+9(g^{(3)})^4+8(g^{(3)})^3}\,, \tag{A1}$$

$$f_1(g^{(2)},g^{(3)})=-\frac{\sqrt[3]{-(g^{(2)})^3+f_0(g^{(2)},g^{(3)})+3g^{(2)}g^{(3)}-3(g^{(3)})^2}}{g^{(3)}} + \frac{18g^{(3)}-9(g^{(2)})^2}{9g^{(3)}\sqrt[3]{-(g^{(2)})^3+f_0(g^{(2)},g^{(3)})+3g^{(2)}g^{(3)}-3(g^{(3)})^2}}+\frac{g^{(2)}}{g^{(3)}}\,, \tag{A2}$$

$$f_2(g^{(3)})=\mathrm{Re}\left(\frac{\sqrt[3]{-8748(g^{(3)})^2-4860g^{(3)}+8748\left(g^{(3)}-\frac{2}{9}\right)^{3/2}\sqrt{g^{(3)}+54}}}{18\sqrt[3]{2}} - \frac{-324g^{(3)}-9}{9\times 2^{2/3}\sqrt[3]{-8748(g^{(3)})^2-4860g^{(3)}+8748\left(g^{(3)}-\frac{2}{9}\right)^{3/2}\sqrt{g^{(3)}+54}}}\right)+\frac{1}{6}\,. \tag{A3}$$

These are reduced density of probability distributions in $\mathcal{H}_3$,

$$\mathcal{P}_g(n_0,g^{(2)})=\begin{cases} 3n_0^2-3n_0^3+\dfrac{3}{2}g^{(2)}n_0^4, & \text{if } g^{(2)}<\dfrac{3}{n_0}-\dfrac{3}{n_0^2}g^{(2)}\le\dfrac{1}{n_0}\,,\\ 3n_0^2-2n_0^3+\dfrac{g^{(2)}n_0^4}{2}, & \text{if } g^{(2)}<\dfrac{3}{n_0}-\dfrac{3}{n_0^2} \text{ and } g^{(2)}>\dfrac{1}{n_0}\,,\\ \dfrac{g^{(2)}n_0^4}{2}, & \text{if } g^{(2)}\ge\dfrac{3}{n_0}-\dfrac{3}{n_0^2} \text{ and } g^{(2)}<\dfrac{1}{n_0}\,,\\ n_0^3-\dfrac{g^{(2)}n_0^4}{2}, & \text{if } g^{(2)}\ge\dfrac{3}{n_0}-\dfrac{3}{n_0^2} \text{ and } g^{(2)}\ge\dfrac{1}{n_0}\,, \end{cases} \tag{A4}$$

$$\mathcal{P}_g(n_0,g^{(3)})=\frac{n_0^5}{2}\begin{cases} \dfrac{2}{n_0^2}-\dfrac{1}{n_0}+\dfrac{n_0g^{(3)}}{6}, & \text{if } g^{(3)}<\dfrac{6-6n_0}{n_0^3-3n_0}\,,\\ -\dfrac{g^{(3)}}{n_0}+\dfrac{1}{n_0}+\dfrac{n_0g^{(3)}}{2}, & \text{if } g^{(3)}\ge\dfrac{6-6n_0}{n_0^3-3n_0} \text{ and } n_0\ge\sqrt{3}\,,\\ \dfrac{2}{n_0^2}-\dfrac{1}{n_0}+\dfrac{n_0g^{(3)}}{6}, & \text{if } g^{(3)}\ge\dfrac{6-6n_0}{n_0^3-3n_0} \text{ and } n_0<\sqrt{3}\,, \end{cases} \tag{A5}$$

$$\mathcal{P}_g(g^{(2)})=\begin{cases} \dfrac{2g^{(2)}\left(\left(-12\sqrt{9-12g^{(2)}}+16\sqrt{1-2g^{(2)}}+75\right)g^{(2)}+63\sqrt{9-12g^{(2)}}-56\sqrt{1-2g^{(2)}}-190\right)-81\sqrt{9-12g^{(2)}}+48\sqrt{1-2g^{(2)}}+195}{60(g^{(2)})^4}, & \text{if } 0\le g^{(2)}\le\frac{1}{2}\,,\\ \dfrac{2g^{(2)}\left(-3\left(4\sqrt{9-12g^{(2)}}-16\sqrt{4-6g^{(2)}}+75\right)g^{(2)}+63\sqrt{9-12g^{(2)}}-224\sqrt{4-6g^{(2)}}+370\right)-81\sqrt{9-12g^{(2)}}+256\sqrt{4-6g^{(2)}}-271}{60(g^{(2)})^4}, & \text{if } \frac{1}{2}<g^{(2)}\le\frac{2}{3}\,,\\ \dfrac{2\sqrt{9-12g^{(2)}}(21-4g^{(2)})g^{(2)}-27\sqrt{9-12g^{(2)}}+5}{10(g^{(2)})^4}, & \text{if } \frac{2}{3}<g^{(2)}\le\frac{3}{4}\,,\\ \dfrac{1}{2(g^{(2)})^4} & \text{if } g^{(2)}>\frac{3}{4}\,. \end{cases} \tag{A6}$$

APPENDIX B: UPPER BOUNDARIES FOR $g^{(k)}$ IN $\mathcal{H}_N$

Proposition 1. Given some $\mathcal{H}_N$, for every pair $G^{(k-1)}$ and $G^{(k)}$ with $k \leq N$, the inequality $(N-k+1)!G^{(k-1)} \geq (N-k)!G^{(k)}$ is satisfied. Subsequently, it holds that $0!G^{(N)} \leq 1!G^{(N-1)} \leq \cdots \leq (N-3)!G^{(3)} \leq (N-2)!G^{(2)}$.

Since these observables can be expressed as

$$G^{(k-1)} = \sum_{n=k-1}^{N} \frac{n!}{(n-k+1)!} P_n \,, \tag{B1a}$$

$$G^{(k)} = \sum_{n=k}^{N} \frac{n!}{(n-k)!} P_n \,, \tag{B1b}$$

it follows that

$$G^{(k-1)} - \frac{(N-k)!}{(N-k+1)!} G^{(k)} = (k-1)! P_{k-1} + \sum_{n=k}^{N} \left(\frac{1}{(n-k+1)!} - \frac{(N-k)!}{(N-k+1)!(n-k)!)} \right) n! P_n \,. \tag{B2}$$

The term in parentheses in the summation is always greater than 0 and is equal to 0 only if $n = N$. Therefore, the right side of the last equation is greater than 0 as well,

$$G^{(k-1)} - \frac{(N-k)!}{(N-k+1)!} G^{(k)} \geq 0 \,, \tag{B3}$$

i.e., $(N-k+1)!G^{(k-1)} \geq (N-k)!G^{(k)}$.

Proposition 2. In every Hilbert space $\mathcal{H}_N$, $g^{(2)}$ admits an upper boundary that is given by $\frac{N-1}{n_0}$.

From the definition for $n_0 = \sum_{n=0}^{N} nP_n$ and $G^{(2)} = \sum_{n=0}^{N} n(n-1)P_n$ in $\mathcal{H}_N$, we find, multiplying n_0 by $N-1$,

$$\sum_{n=0}^{N} n(N-1)P_n = (N-1)P_1 + \cdots + N(N-1)P_N \,. \tag{B4}$$

Subtracting $G^{(2)}$ from expression (B4) leads to $\sum_{n=0}^{N} n(N-n)P_n$. This is always greater than 0 and only equal if every term of the summation is null since all of them are positive (remembering that $1 \geq P_n \geq 0$). Therefore

$$(N-1)n_0 \geq G^{(2)} \,, \tag{B5}$$

or since $G^{(2)} = n_0^2 g^{(2)}$,

$$g^{(2)} \leq \frac{N-1}{n_0} \,. \tag{B6}$$

Finally, $g^{(2)}$ can reach its upper boundary only if every P_n vanishes except P_0 and P_N, i.e., when the corresponding state is a "Coin state," cf. Eq. (23). Assuming both propositions, we can infer that

$$G^{(k)} \leq \frac{(N-2)!}{(N-k)!} G^{(2)} \,. \tag{B7}$$

Furthermore, as $G^{(k)}$ can be written as $n_0^k g^{(k)}$ and from Eq. (B6), we obtain

$$g^{(k)} \leq \frac{(N-2)!}{(N-k)!} \frac{g^{(2)}}{n_0^{k-2}} \leq \frac{(N-1)!}{(N-k)!} \frac{1}{n_0^{k-1}} \,. \tag{B8}$$

[1] J. von Neumann, *Mathematical Foundations of Quantum Mechanics* (Princeton University Press, 1932).
[2] W. Heisenberg, Z. Phys. **33**, 879 (1925).
[3] E. Schrödinger, Phys. Rev. **28**, 1049 (1926).
[4] S. C. Bloch, *Introduction to Classical and Quantum Harmonic Oscillators* (Wiley-Interscience, 1997).
[5] R. J. Glauber, Rev. Mod. Phys. **78**, 1267 (2006).

[6] W.-M. Zhang, D. H. Feng, and R. Gilmore, Rev. Mod. Phys. **62**, 867 (1990).
[7] E. C. G. Sudarshan, Phys. Rev. Lett. **10**, 277 (1963).
[8] R. J. Glauber, Phys. Rev. Lett. **10**, 84 (1963).
[9] A. I. Lvovsky, H. Hansen, T. Aichele, O. Benson, J. Mlynek, and S. Schiller, Phys. Rev. Lett. **87**, 050402 (2001).
[10] D. T. Pegg and S. M. Barnett, Europhys. Lett. **6**, 483 (1988).
[11] J. C. López Carreño, C. Sánchez Muñoz, D. Sanvitto, E. del Valle, and F. P. Laussy, Phys. Rev. Lett. **115**, 196402 (2015).
[12] J. C. López Carreño and F. P. Laussy, Phys. Rev. A **94**, 063825 (2016).
[13] C. Sánchez Muñoz, E. del Valle, A. G. Tudela, K. Müller, S. Lichtmannecker, M. Kaniber, C. Tejedor, J. Finley, and F. Laussy, Nat. Photonics **8**, 550 (2014).
[14] X.-B. Wang, T. Hiroshima, A. Tomita, and M. Hayashi, Phys. Rep. **448**, 1 (2007).
[15] G. Breitenbach, S. Schiller, and J. Mlynek, Nature **387**, 471 (1997).
[16] D. Leibfried, E. Knill, S. Seidelin, J. Britton, R. Blakestad, J. Chiaverini, D. Hume, W. Itano, J. Jost, C. Langer *et al.*, Nature **438**, 639 (2005).
[17] V. Dodonov, I. Malkin, and V. Man'ko, Physica **72**, 597 (1974).
[18] H. P. Yuen, Phys. Rev. A **13**, 2226 (1976).
[19] G. S. Agarwal and K. Tara, Phys. Rev. A **43**, 492 (1991).
[20] Z.-Z. Xin, Y.-B. Duan, H.-M. Zhang, M. Hirayama, and K.-i. Matumoto, J. Phys. B: At., Mol. Opt. Phys. **29**, 4493 (1996).
[21] W. Wu and L.-A. Wu, J. Math. Phys. **45**, 1752 (2004).
[22] D. Stoler, B. Saleh, and M. Teich, Opt. Acta **32**, 345 (1985).
[23] K. Matsuo, Phys. Rev. A **41**, 519 (1990).
[24] A. Othman, in Photonics North (PN), 2016.
[25] R. J. Glauber, Phys. Rev. **131**, 2766 (1963).
[26] L. Susskind and J. Glogower, Physics **1**, 49 (1964).
[27] J. H. Shapiro and S. R. Shepard, Phys. Rev. A **43**, 3795 (1991).
[28] M. J. W. Halls, J. Mod. Opt. **40**, 809 (1993).
[29] S. M. Barnett and P. M. Radmore, *Methods in Theoretical Quantum Optics* (Oxford University Press, 1997).
[30] T. C. H. Liew, Y. G. Rubo, A. S. Sheremet, S. D. Liberato, I. A. Shelykh, F. P. Laussy, and A. V. Kavokin, New J. Phys. **18**, 023041 (2016).
[31] M. A. Nielsen and I. L. Chuang, *Quantum Computation and Quantum Information* (Cambridge University Press, 2000).
[32] P. Michler, A. Kiraz, C. Becher, W. V. Schoenfeld, P. M. Petroff, L. Zhang, E. Hu, and A. Ĭmamoḡlu, Science **290**, 2282 (2000).
[33] S. Dong, T. Huang, Y. Liu, J. Wang, G. Zhang, L. Xiao, and S. Jia, Phys. Rev. A **76**, 063820 (2007).
[34] V. B. Verma, M. J. Stevens, K. L. Silverman, N. L. Dias, A. Garg, J. J. Coleman, and R. P. Mirin, Opt. Express **19**, 4182 (2011).
[35] G. D. Martino, Y. Sonnefraud, S. Kéna-Cohen, M. Tame, Ş. K. Özdemir, M. S. Kim, and S. A. Maier, Nano Lett. **12**, 2504 (2012).
[36] M. E. Reimer, G. Bulgarini, N. Akopian, M. Hocevar, M. B. Bavinck, M. A. Verheijen, E. P. Bakkers, L. P. Kouwenhoven, and V. Zwiller, Nat. Commun. **3**, 737 (2012).
[37] M. Leifgen, T. Schröder, F. Gädeke, R. Riemann, V. Métillon, E. Neu, C. Hepp, C. Arend, C. Becher, and K. Lauritsen, New J. Phys. **16**, 023021 (2014).
[38] J. C. López Carreño, E. Zubizarreta Casalengua, E. del Valle, and F. P. Laussy, e-print arXiv:1610.06126 (2016).